

FIGURE 42.1 Hypothetical N-terminal loop-flip conformation of fibril-incorporated LC proteins: (A) structure of $\kappa 4$ Len (1–22) from x-ray crystallographic studies; (B) hypothetical type VI β -turn anchored by the proline at position 8 that juxtaposes residues 1–4 and 11–15, which constitute the epitope recognized by the 11-1F4 mAb. (From [29].)

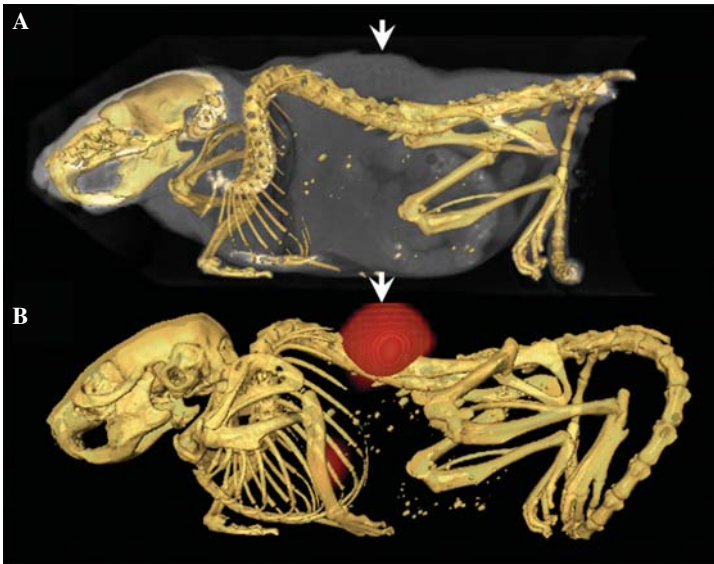


FIGURE 42.2 Immunoimaging of human AL amyloidoma in mice using radioiodinated 11-1F4 mAb: (A) x-ray CT image showing the subcutaneous AL amyloidoma (arrow); (B) the [^{125}I]11-1F4 accumulated in the intrascapular human AL amyloidoma 3 days after injection, as evidenced in co-registered SPECT/CT images. (From [33].)

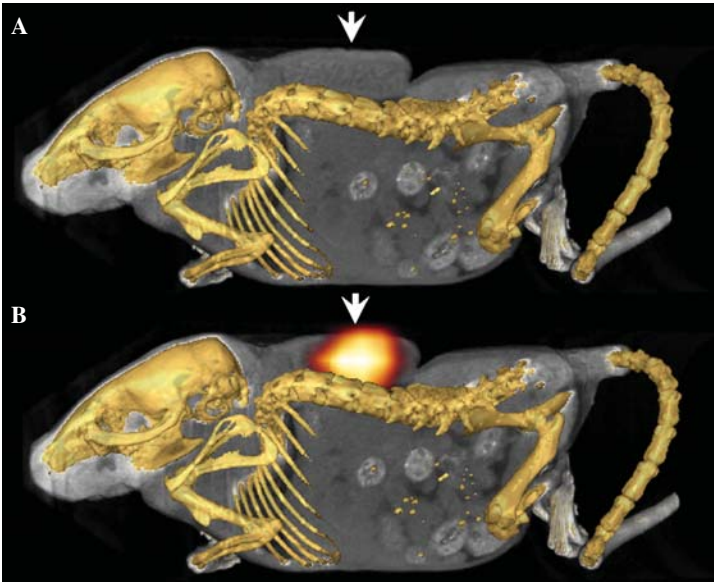


FIGURE 42.3 Immunoinaging of human AL amyloidoma in mice using radioiodinated-enriched IGIV Ab: (A) x-ray CT image showing the subcutaneous AL amyloidoma (arrow); (B) the $[^{125}\text{I}]\text{IGIV}$ accumulated in the human amyloidomas, as evidenced in co-registered SPECT/CT images.

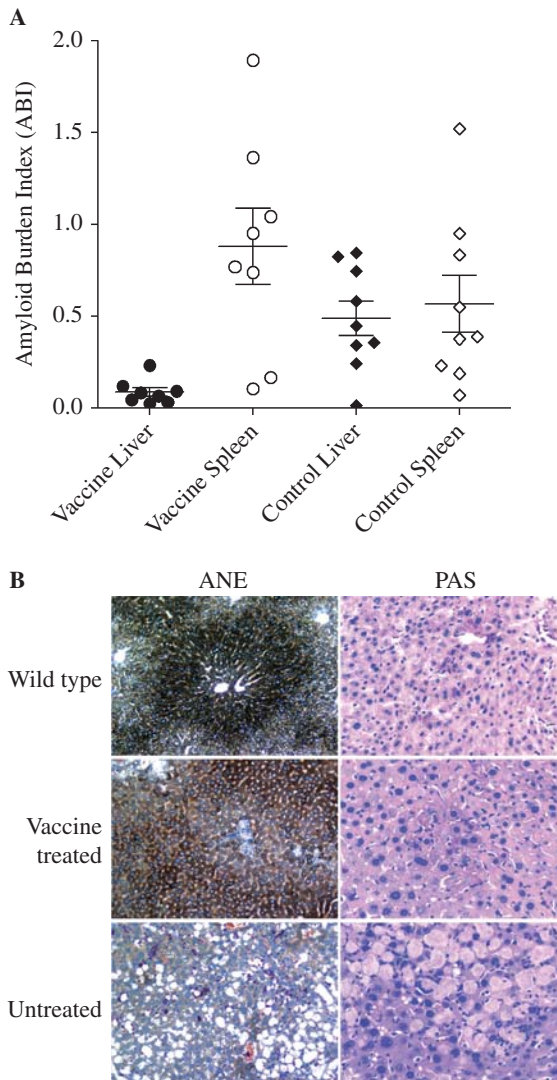


FIGURE 42.4 Manifestation of heterogeneous immunization in mice with AA amyloidosis. (A) Amyloid burden in the liver and spleen of immunized and untreated mice. ABI was calculated by measuring the area occupied by Congo Red birefringent material in formalin fixed tissue sections using Image Pro-Plus visualization software. (B) Histological evaluation of hepatocyte integrity using naphthol AS-D chloroacetate esterase (ANE) and periodic acid Schiff (PAS). Original magnification $\times 160$.